J. Biochem. 2011;150(5):569–577 doi:10.1093/jb/mvr101

JB THE JOURNAL OF BIOCHEMISTRY

Interaction of a goose-type lysozyme with chitin oligosaccharides as determined by NMR spectroscopy

Received April 26, 2011; accepted July 15, 2011; published online August 22, 2011

Shoko Shinya[1,*], Takayuki Ohnuma[1,*], Shunsuke Kawamura[2], Takao Torikata[2], Shigenori Nishimura[3], Etsuko Katoh[4] and Tamo Fukamizo[1,†]

[1]Department of Advanced Bioscience, Kinki University, 3327-204, Nakamachi, Nara 631-8505, Japan; [2]Department of Bioscience, School of Agriculture, Tokai University, Aso, Kumamoto, 869-1404 Japan; [3]Graduate School of Life and Environmental Sciences, Osaka Prefecture University, 1-1 Gakuen-cho, Nakaku, Sakai, Osaka, 599-8531 Japan; and [4]National Institute of Agrobiological Sciences, Tsukuba, Japan

*These authors contributed equally for this work.

†Tamo Fukamizo, Department of Advanced Bioscience, Kinki University, 3327-204, Nakamachi, Nara 631-8505, Japan. Tel: +81-742-43-8237, Fax: +81-742-43-8976, email: fukamizo@nara.kindai.ac.jp

The interaction between a goose-type lysozyme from ostrich egg white (OEL) and chitin oligosaccharides [$(GlcNAc)_n$ ($n = 2$, 4 and 6)] was studied by nuclear magnetic resonance (NMR) spectroscopy. A stable isotope-labelled OEL was produced in *Pichia pastoris*, and backbone resonance assignments for the wild-type and an inactive mutant (E73A OEL) were achieved using modern multi-dimensional NMR techniques. NMR titration was performed with $(GlcNAc)_n$ for mapping the interaction sites of the individual oligosaccharides based on the shifts in the two-dimensional heteronuclear single quantum correlation (HSQC) resonances. In wild-type OEL, the interaction sites for $(GlcNAc)_n$ were basically similar to those determined by X-ray crystallography. In E73A OEL, however, the interaction sites were spread more widely over the substrate-binding cleft than expected, due to the multiple modes of binding. The association constant for E73A OEL and $(GlcNAc)_6$ calculated from the shifts in the Asp97 resonance (7.2×10^3 M^{-1}) was comparable with that obtained by isothermal titration calorimetry (5.3×10^3 M^{-1}). The interaction was enthalpy-driven as judged from the thermodynamic parameters ($\Delta H = -6.1$ kcal/mol and $T\Delta S = -1.0$ kcal/mol). This study provided novel insights into the oligosaccharide binding mechanism and the catalytic residues of the enzymes belonging to family GH-23.

Keywords: goose-type lysozyme/ITC/NMR/oligosaccharide/protein–carbohydrate interaction.

Abbreviations: GEWL, goose egg white lysozyme; GLAc, goose-type lysozyme from Atlantic cod; GlcNAc, *N*-acetyl-D-glucosamine; $(GlcNAc)_n$, β-1,4-linked oligosaccharide of GlcNAc with a polymerization degree of n; HSQC, two-dimensional heteronuclear single quantum correlation; ITC, isothermal titration calorimetry; NMR, nuclear magnetic resonance; OEL, goose-type lysozyme from ostrich egg white.

Lysozyme (E.C. 3.2.1.14) is a lytic enzyme, which hydrolyses the β-1,4-glycosidic linkage between *N*-acetylmuramic acid (MurNAc) and *N*-acetyl-D-glucosamine (GlcNAc) of the peptideglycan chains in bacterial cell walls (*1*, *2*). Among the various types of lysozymes isolated and characterized to date, the enzyme obtained from hen egg white has been studied most intensively with respect to structure and function. Hen egg white lysozyme can hydrolyse chitin [$(GlcNAc)_n$] in addition to cell wall polysaccharide (*3*) and also catalyses significantly, the transglycosylation of oligosaccharide fragments (*4*). Such enzymatic activities have been found in chicken-type (c-type) lysozymes including human lysozyme (*5*) and various avian egg white lysozymes (*6*). For goose-type (g-type) and phage-type lysozymes, however, chitin hydrolytic activity is not detected or found to be very weak (*7*–*9*). No transglycosylation activity has been found for these types of lysozymes (*10*, *11*). Based on the amino acid sequences, c-type, g-type and phage-type lysozymes are classified into family GH-22, family GH-23 and family GH-24, respectively (*12*). The catalytic cleft of these enzymes is formed by a structurally invariant core consisting of three α-helices and a three-stranded β-sheet (*13*). The c-type enzymes are retainer, whereas, the g-type and phage-type enzymes are inverter. Structural determinants for substrate recognition and for the transglycosylation activity are considered to lie in the substrate-binding and catalytic cleft of these lysozymes. Thus, a comparison between the fine structure of the substrate-binding cleft of these enzymes would provide insights into the mechanism of substrate recognition and catalysis of the enzymes belonging to the lysozyme superfamily.

Crystal structures of goose egg white lysozyme (GEWL) and its complex with $(GlcNAc)_3$ have been reported by Weaver *et al.* (*14*, *15*), and the trisaccharide was found to bind to subsites B, C and D (−3, −2 and −1) of the enzyme. Recently, the crystal structure analysis of a g-type lysozyme from Atlantic cod in a complex with both $(GlcNAc)_2$ and $(GlcNAc)_3$ revealed the substrate-binding mode at subsites E, F and G (+1, +2 and +3) in addition to that at subsites B–D (*16*). On the other hand, GEWL hydrolyses predominantly the mid linkage of $(GlcNAc)_6$, producing two

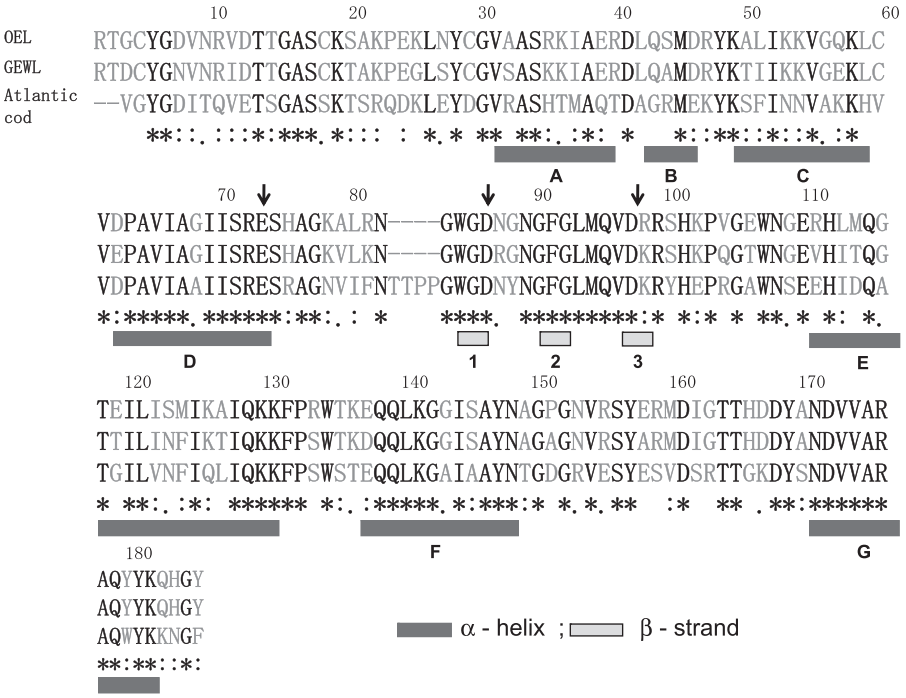

Fig. 1 Amino acid sequence alignment of goose-type lysozymes from ostrich egg white (OEL), goose egg white (GEWL) and Atlantic cod (GLAc). The residues completely conserved are marked by asterisks. Catalytic residues are indicated by arrows. The secondary structures of the crystal form of GEWL in a complex with $(GlcNAc)_3$ are also aligned with the primary structure.

molecules of $(GlcNAc)_3$ (*17*), indicating that $(GlcNAc)_6$ binds to the entire substrate-binding cleft, −3, −2, −1, +1, +2 and +3, of GEWL upon its hydrolysis. Thus, it is highly desirable to examine the binding of $(GlcNAc)_6$ to g-type lysozymes for analysing the most productive mode of binding leading to hydrolysis. Kawamura *et al.* (*18*) reported the efficient expression of a g-type lysozyme from ostrich egg white (OEL) using *Pichia pastoris*. This system would enable a level of production of ^{13}C- or ^{15}N-labelled OEL sufficient for nuclear magnetic resonance (NMR) measurements. The amino acid sequence of OEL is 83% homologous to that of goose egg white lysozyme, as shown in Fig. 1 (*19*). The enzymatic properties of OEL are almost identical with those of goose egg white lysozyme (*18*).

In the present study, we produced OEL and a catalytic residue(Glu73)-deficient mutant with the *P. pastoris* expression system, and stable isotope-labelled OELs were employed for oligosaccharide-binding experiments using NMR spectroscopy. Isothermal titration calorimetry (ITC) was also used for determining quantitatively the oligosaccharide-binding to OEL.

Experimental procedures

Materials

N-acetylglucosamine oligosaccharides $[(GlcNAc)_n,\ n=1–6]$ were purchased from Seikagaku Kogyo Co. (Tokyo, Japan). The *P. pastoris* expression system including expression vector pPIC9K was purchased from Invitrogen (Carlsbad, CA, USA). The *P. pastoris* GS115 (Invitrogen) was used as the host strain for expression. ^{15}N-ammonium chloride, ^{13}C-D-glucose and ^{13}C-methanol were obtained from Cambridge Isotope Laboratories Inc. (Andover, MA, USA). Other reagents were of analytical grade available commercially.

Production of OEL and its mutant enzymes

A recombinant OEL and inactive mutant (E73A OEL) with an extra serine residue at the N-terminus were obtained as described previously (*20*). It has been reported that the additional serine residue at the N-terminus had little effect on the secondary structure, substrate-binding ability, lytic activity and structural stability of OEL (*20*, *21*). E73D and E73Q were not employed in this study, because E73D has a small extent of the enzymatic activity and the stability of E73Q is the lowest among the Glu73-mutated enzymes (*20*). The recombinant OEL enzymes with an extra N-terminal serine was used throughout this study.

Production of ^{15}N-labelled OEL and ^{15}N-/^{13}C-labelled OEL

A recombinant *P. pastoris* clone harbouring an expression plasmid for the wild-type or its derivative was typically inoculated into 3 ml of FM22-glycerol medium [4.29% KH_2PO_4, 0.1% $CaSO_4{\cdot}2H_2O$, 1.17% $MgSO_4{\cdot}7H_2O$, 1.43% K_2SO_4, 0.34% KOH, 1% glycerol, 6×10^{-5}% biotin, 0.1% (v/v) PTM1 salts and 0.1% $^{15}NH_4Cl$] and then incubated at 30°C for 48 h. This seed culture was subcultured into 200 ml of the same medium for an additional 48 h. The cells were harvested and then transferred to 900 ml of the same medium containing 0.5% (v/v) methanol instead of glycerol to give an OD_{600} of 1.0 to induce production. The culture was maintained for 120 h with methanol supplementation to a final concentration of 0.5% every 24 h. The ^{15}N-labelled protein secreted into the culture supernatant was purified by successive cation-exchange chromatographies as described previously (*20*). The purity was confirmed by SDS–PAGE. The N-terminal amino acid sequence was determined with a Shimadzu model PPSQ21 sequencer. The expression and purification of $^{13}C/^{15}N$-labelled proteins were performed as described above, except that FMGY medium (same as FM22-glycerol medium but containing 5% ^{13}C-glucose instead of 1% glycerol) and FMMY medium [same as FMGY medium but containing 0.5% (v/v) ^{13}C-methanol instead of 5% ^{13}C-glucose] were used for growing *P. pastoris* and for induction of proteins, respectively.

Sequential assignment of the backbone signals of OEL

NMR samples contained 0.2–0.5 mM protein in 20 mM sodium acetate buffer pH 5.0 (90% H_2O/10% D_2O). All NMR spectra were acquired at 298 K using a Bruker AV500 spectrometer controlled with TopSpin 3.0 software and equipped with a triple-resonance pulsed-field-gradient cryoprobe head.

^{1}H chemical shifts were referenced to HDO (4.64 ppm at 30°C) relative to 3-(trimethylsilyl) 3,3,3,3-tetradeutero-propionic acid (TSP). ^{15}N and ^{13}C chemical shifts were indirectly calibrated from each gyromagnetic ratio (*22*). Sequential assignments were performed using ^{15}N/^{13}C-labelled OEL from two-dimensional ^{1}H-^{15}N two-dimensional heteronuclear single quantum correlation (HSQC) and from three-dimensional HNCACB, CBCA(CO)NH, HNCA, HNCACO, HNCO and HNCOCA experiments; analysis of these spectra resulted in the nearly complete assignment of the backbone ^{1}H, ^{13}C and ^{15}N resonances. All spectra were processed using NMRPipe software (*23*) and were analysed using Sparky software (*24*).

Titration of $(GlcNAc)_n$ ($n = 2$, 4 and 6)

Two-dimensional ^{1}H-^{15}N HSQC spectra were recorded for 0.25 mM ^{15}N-labelled OEL in 50 mM sodium acetate pH 5.0 (90% H_2O/10%D_2O), in the presence of various concentrations of $(GlcNAc)_n$. Chemical shift changes induced by the oligosaccharide binding ($\Delta\delta$) were calculated by the equation,

$$\Delta\delta = \left[\left(\Delta NH^2 + \Delta N^2/25\right)/2\right]^{1/2}$$

where ΔNH and ΔN represent the observed shifts in the ^{1}H-axis and ^{15}N-axis, respectively. Since the interaction between the enzyme and $(GlcNAc)_6$ was a slow exchange, $\Delta\delta$ values could not be determined for individual titration points. Thus, the relative intensity of the bound state to the total intensity of the free and bound states [$I_{bound}/(I_{free} + I_{bound})$] was plotted against the free oligosaccharide concentrations, and the association constant, K_{assoc}, was estimated by non-linear curve fitting based on the equation,

$$I_{bound}/(I_{free}+I_{bound}) = [S]_{free}/\left([S]_{free}+1/K_{assoc}\right)$$

The free oligosaccharide concentrations $[S]_{free}$ were obtained by subtracting the bound oligosaccharide concentration [ES] from the total oligosaccharide concentration $[S]_{total}$.

ITC experimnents

ITC was performed with a MicroCal VP-ITC calorimeter. The instrument's design and its operation have been described in detail elsewhere (*25*). The OEL samples used in these experiments were prepared by first dialysing for ~16 h against 20 mM sodium acetate buffer, pH 5.0. $(GlcNAc)_6$ was dissolved in the same buffer. For a given experiment, 7 µl aliquots of 9.65–31.9 mM $(GlcNAc)_6$ in 20 mM sodium acetate buffer, pH 5.0, were added via a 250 µl syringe to a sample cell that contained 1.4482 ml of a stirred (310 rpm) 178–364 µM OEL solution equilibrated at 30°C. After each injection, the amount of heat released was measured. Prior to experimentation, the instrument containing water in the sample and reference cells was equilibrated overnight. Stable base lines were defined as those with root mean square noise levels of less than 5 ncal s^{-1}. The heat of dilution caused by an injection of $(GlcNAc)_6$ was measured with the same buffer, injection and temperature, but by adding ligand to a sample solution lacking protein. The heat of dilution was subtracted from the heat change that occurred when protein was present. Non-linear fitting of the data was performed using MicroCal Origin 7.0 (Origin-Lab Corp.). The parameters that were varied to minimize the standard deviation of the fit to the experimental data were the binding constant (K_{assoc}), the enthalpy change (ΔH) and the number of binding sites per protein molecule (stoichiometry; n). The derived values for K_{assoc}, ΔH, and n at 30°C were then used to calculate the changes in free energy (ΔG) and entropy (ΔS).

Results and discussion

Protein production and purification

We previously developed an efficient expression system for the recombinant OEL with an extra N-terminal serine residue in the methylotropic yeast *P. pastoris* (*18*). Furthermore, using this system, we generated a Glu73-mutated protein (E73A), in which Glu73 was substituted with Ala and demonstrated the involvement of Glu73 as a critical catalytic residue in g-type lysozyme (*20*). Since E73A OEL was virtually inactive with little change in the Circular dichroism (CD) spectrum (secondary structure), we considered it most appropriate for the study of the substrate-binding mechanism of g-type lysozymes. Therefore, using the *P. pastoris* system, we produced ^{15}N-labelled and ^{13}C/^{15}N-labelled wild-type and E73A OELs for NMR experiments.

The ^{15}N-labelled and ^{13}C/^{15}N-labelled proteins were successfully expressed and secreted into the culture medium. The purified proteins were found to give a single band on SDS–PAGE and a single symmetrical peak on cation exchange chromatography (Supplementary Fig. S1). The N-terminal sequence of each protein was determined to be Ser-Arg-Thr-Gly-, indicating that the protein was correctly processed at the C-terminus of the α-factor signal. A quantity of ~35–40 mg of the ^{15}N-labelled and ^{13}C/^{15}N-labelled proteins, which is sufficient for heteronuclear NMR measurements, were obtained from 1 l of yeast culture. The enzymatic activity and CD spectra of the ^{15}N-labelled and ^{13}C/^{15}N-labelled proteins were identical with those of the corresponding non-labelled proteins (Supplementary Figs S2 and S3).

HSQC spectra of the wild-type and E73A OEL

The HSQC spectrum of the wild-type OEL exhibited well dispersed and intense signals as shown in Fig. 2. Most backbone resonances were assigned sequentially by means of a combination of three-dimensional NMR experiments using ^{15}N/^{13}C-labelled OEL. These assignments are given in Fig. 2. However, the backbone resonances for Tyr157–Asp161 could not be assigned, because of the line-broadening of the amide protons due to the rapid exchange with the solvent. The HSQC spectrum of E73A OEL was almost identical with that of the wild-type OEL, and the backbone resonances were assigned by a similar manner to that for the wild-type. As shown in Fig. 3, most amino acids affected by the mutation were found to be located near or inside the catalytic cleft, except Ile119. The effect on the Ile119 resonance might be a secondary effect derived from the conformational change in the catalytic cleft. NMR assignment data obtained in this study have been deposited into Biological Magnetic Resonance Data Bank (BMRB) (code numbers, 11434 and 11436).

NMR titration with the substrate analogues using the wild-type OEL

When $(GlcNAc)_2$ was added to the wild-type OEL solution in a saturated condition [OEL, 0.28 mM; $(GlcNAc)_2$, 14.3 mM], only a minor shift was observed in the resonance of Val96, which is located in the $(GlcNAc)_3$ binding region of GEWL as determined by X-ray crystallography (*15*) (Fig. 4A). The shift in Val96 was enhanced, and the influence extended to neighbouring amino acids, such as Arg99, Ser100, Asn148, Ala149, Gly150 and Thr165, upon addition of $(GlcNAc)_4$ instead of $(GlcNAc)_2$ [OEL, 0.28 mM; $(GlcNAc)_4$, 14.3 mM; Fig. 4B]. Notably, the resonances for Arg99 and Thr165 completely disappeared upon the addition of $(GlcNAc)_4$. The influences on the spectrum were not further enhanced upon the

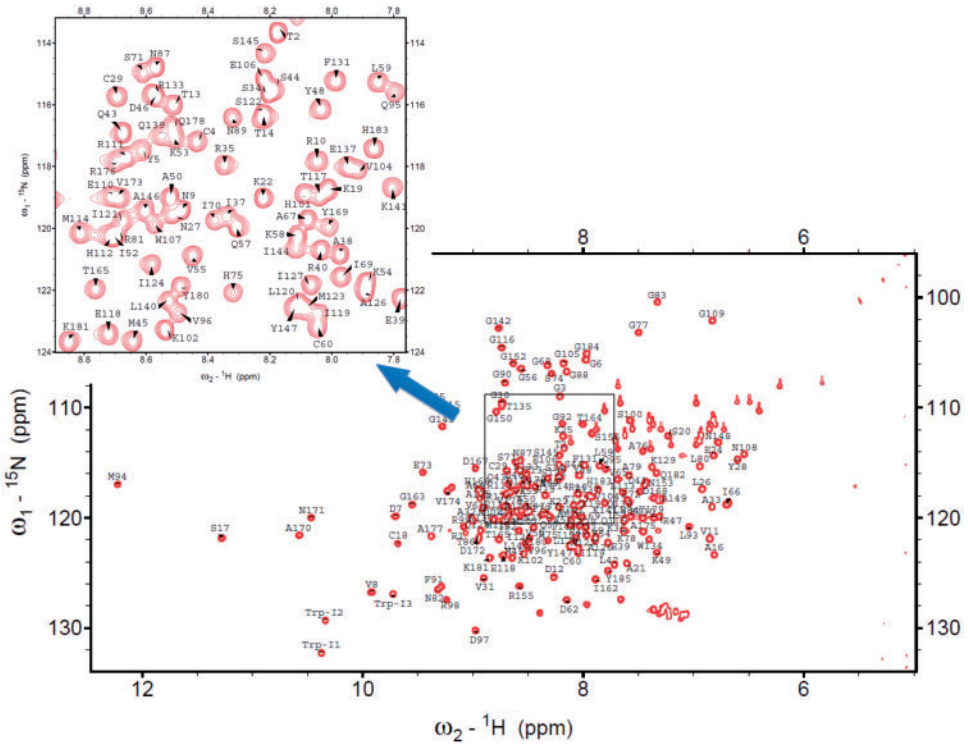

Fig. 2 ^{1}H-^{15}N-HSQC spectrum of the wild-type OEL. The protein was dissolved in 20 mM sodium acetate buffer pH 5.0 containing 10% D_2O to obtain 0.2 mM OEL solution. The backbone resonances were assigned in a sequential manner as labelled for the individual resonances. The side chain resonances were not assigned in this study. An enlargement of the boxed region of the spectrum is also shown in the upper-left panel.

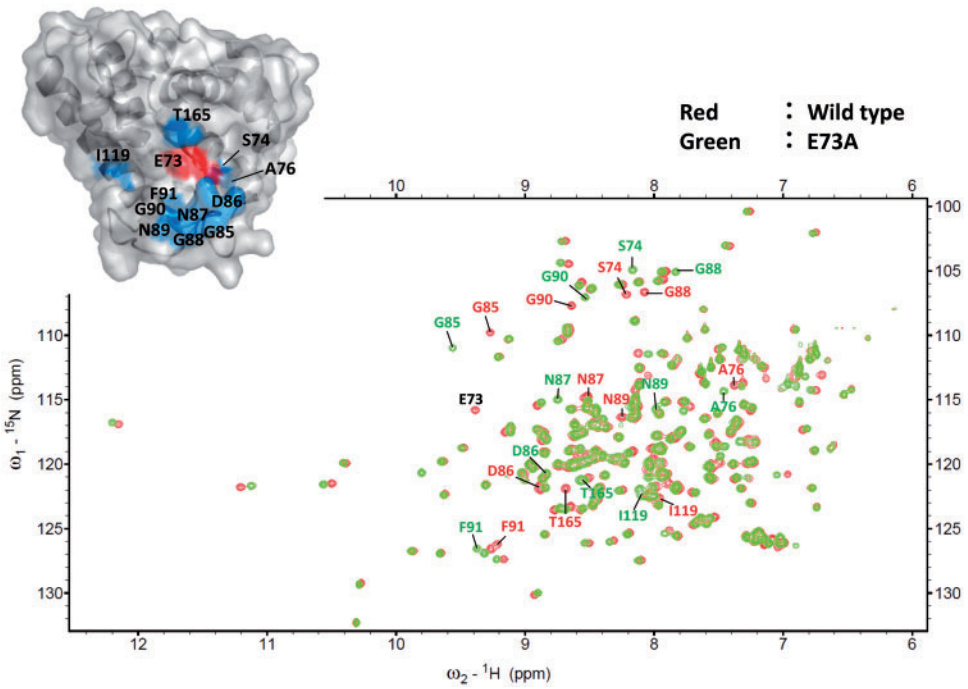

Fig. 3 Superimposition of the ^{1}H-^{15}N-HSQC spectra of the wild-type and E73A OEL. The resonances affected by the E73A mutation ($\Delta\delta > 0.1$ ppm) are labelled in the spectrum. The amino acid residues, of which the resonances are affected, are mapped in the GEWL molecule (PDB code: 154 L) in blue. The mutated Glu73 is in red.

addition of $(GlcNAc)_6$ (data not shown), due to the enzymatic hydrolysis of $(GlcNAc)_6$ to $(GlcNAc)_3$ (*17*). A small fraction of $(GlcNAc)_4$ would also be hydrolysed into $(GlcNAc)_2$ by OEL (Fig. 4B). However, since the effect of $(GlcNAc)_2$ on the spectrum was very small (Fig. 4A), the data for $(GlcNAc)_4$ titration would reflect mostly the conformational changes induced by $(GlcNAc)_4$ binding.

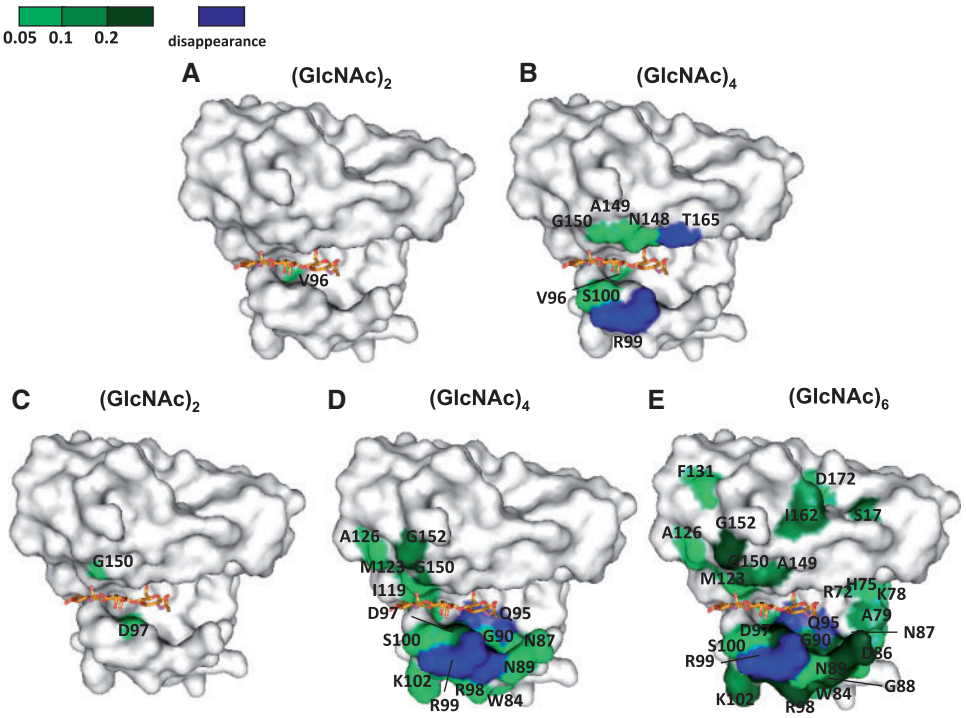

Fig. 4 Amino acid residues affected by oligosaccharide binding to wild-type OEL (A and B) and to E73A OEL (C–E). The residues, whose amide backbone resonances were significantly affected by oligosaccharide binding ($\Delta\delta > 0.05$ ppm), are shown in green using the surface model of the crystal structure of GEWL in a complex with $(GlcNAc)_3$ (PDB code: 154 L). The bound $(GlcNAc)_3$ in the crystal structure is represented by a stick model. The individual residues are −3, −2 and −1 sugars from the left. Amino acid residues, whose resonances were not detected because of the intensive broadening as a consequence of the oligosaccharide binding, are coloured indigo-blue. Concentration of wild-type OEL was 0.28 mM, and the ligands were 15 mM $(GlcNAc)_2$ (A) and 15 mM $(GlcNAc)_4$ (B). Concentration of E73A OEL was 0.31 mM, and the ligands were. 2.9 mM $(GlcNAc)_2$ (C), 1.7 mM $(GlcNAc)_4$ (D) and 1.7 mM $(GlcNAc)_6$ (E).

NMR titration with substrate analogues using E73A OEL

To examine the binding mode of $(GlcNAc)_6$, we used the inactive mutant, E73A OEL, instead of the wild-type OEL for the titration experiments. The shifts of the HSQC resonances resulting from the chitin oligosaccharide binding were enhanced in E73A OEL as compared with the wild-type, as shown in Fig. 4C–E. Upon the titration of $(GlcNAc)_2$, significant shifts were observed in the resonances for Asp97 and Gly150 (Fig. 4C) in the saturated condition [E73A OEL, 0.28 mM; $(GlcNAc)_2$, 2.9 mM]. Saturation of E73A OEL with $(GlcNAc)_4$ [E73A OEL, 0.33 mM; $(GlcNAc)_4$, 1.7 mM] shifted the resonances of amino acids located in the upper-left region of the binding cleft (residues Ile119, Met123, Ala126, Gly150, Gly152) in addition to the bottom β-stranded region (residues 86–102) (Fig. 4D). The exchange rate between the free and bound states of E73A OEL was fast with respect to the NMR time scale. The regions affected by $(GlcNAc)_4$ were greater in E73A OEL than the wild-type (Fig. 4B). Asn148, Ala149 and Thr165 are affected by the binding of $(GlcNAc)_4$ in the wild-type enzyme but not in E73A OEL. On the other hand, the upper-left region of the binding cleft, including the residues Ile119, Met123, Ala126, Gly150, Gly152, is affected by the binding of $(GlcNAc)_4$ to E73A OEL, but not to the wild-type. Non-productive binding of $(GlcNAc)_4$ to the glycon binding site (subsites −4, −3, −2 and −1) might be enhanced, due to the lack of interaction between the −1 sugar and Glu73. The difference in the $(GlcNAc)_4$ binding mode between wild-type OEL and E73A OEL suggests a risk of using the catalytic residue-deficient mutant for binding experiments. The data obtained by the mutants might not always reflect the interaction of the wild-type protein. However, the risk would be reduced when the longer chain-length oligosaccharides, which can occupy the entire substrate-binding cleft, such as $(GlcNAc)_6$, are used for the binding experiments.

On saturation with $(GlcNAc)_6$ [E73A OEL, 0.33 mM; $(GlcNAc)_6$, 1.7 mM], the chemical shift changes of the 87th, 98th and 152nd residues were further enhanced as compared with the $(GlcNAc)_4$ titration, and the regions affected by the oligosaccharide spread to cover the entire substrate-binding cleft including residues located outside the cleft (Ser17, Ile162 and Asp172) as shown in Fig. 4E. The polypeptide regions containing these residues appear to be in contact with the chains forming the binding cleft within the hydrophobic core, as judged from the crystal structure of GEWL. This situation would have resulted in the conformational changes in the regions outside the cleft, especially in E73A OEL, to which $(GlcNAc)_6$ more tightly binds than to the wild-type. However, more definitive discussion should be done based on the crystal structure of OEL, which has not been reported yet. The exchange between the free and

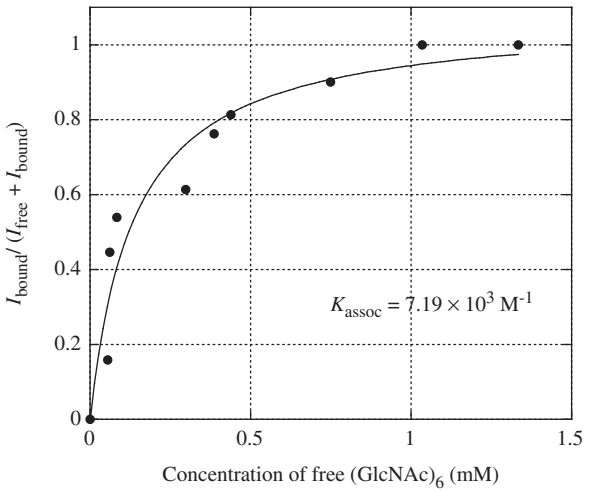

Fig. 5 Titration curve of $(GlcNAc)_6$ binding to E73A OEL determined from the change in the amide backbone resonance of Asp97. The individual experimental points were obtained from integrals of the resonances in the free and bound states using the equation $I_{bound}/(I_{free}+I_{bound})$. The solid line indicates the theoretical binding curve best fitted to the experimental points.

bound states slowed upon the addition of $(GlcNAc)_6$. It is likely that $(GlcNAc)_6$ binds to E73A OEL more tightly than $(GlcNAc)_4$ and $(GlcNAc)_2$ do. We did not observe any change in the resonances for amino acids located at the back of the binding cleft. These effects are clearly dependent upon the degree of polymerization of the $(GlcNAc)_n$ added. However, it should be considered that shifts of the HSQC resonances resulting from the oligosaccharide binding are derived not from a specific mode of binding but from the total effects of several binding modes. $(GlcNAc)_n$ can interact with E73A OEL through multiple modes of binding;e.g. a fraction of $(GlcNAc)_4$ binds to subsites -4, -3, -2 and -1, and the other fraction binds to subsites -2, -1, $+1$ and $+2$. Thus, the conformational changes induced by $(GlcNAc)_n$ binding appear to spread widely over the substrate-binding cleft.

For determination of the association constant for $(GlcNAc)_6$ and E73A OEL, relative increases in the intensity of the Asp97 resonance of the $(GlcNAc)_6$-bound state $[I_{bound}/(I_{bound}+I_{free})]$ were calculated from the individual titration spectra, and plotted against the free oligosaccharide concentration. The result is shown in Fig. 5. The association constant was calculated to be $7.2 \times 10^3\ M^{-1}$.

ITC experiments

ITC experiments were conducted to confirm the binding data obtained by NMR spectroscopy. The association constant (K_{assoc}), the enthalpy change for binding (ΔH) and the stoichiometry of the complex (n) were obtained for interaction between E73A OEL and $(GlcNAc)_6$ by ITC (*26*, *27*). Figure 6 shows the results for an ITC experiment when 3.5-μl portions of 10 mM $(GlcNAc)_6$ were titrated into a 1.4482-ml solution containing 53 μM E73A OEL in 20 mM sodium acetate, pH 5.0. In Fig. 6A, the area within each trough is a measure of the heat released upon the addition of $(GlcNAc)_6$. Figure 6B is a plot of the heat released, normalized to 1 mol of the oligosaccharide, versus the molar ratio of E73A OEL to $(GlcNAc)_6$. The theoretical 'best fit' binding curves are also shown in Fig. 6B. When n was free to vary during fitting, the data were best fit with a stoichiometry of ~1.0 for E73A OEL. The association constant was calculated to be $5.3 \times 10^3\ M^{-1}$. The value is comparable with that obtained by NMR titration (Fig. 5). The interaction between E73A and $(GlcNAc)_6$ was estimated to be enthalpy-driven from the thermodynamic parameters, $\Delta H = -6.1$ kcal/mol and $T\Delta S = -1.0$ kcal/mol ($\Delta S = -3.2$ cal/K·mol). The binding free energy change (ΔG) was -5.1 kcal/mol. Honda and Fukamizo (*17*) reported the binding free energy changes of individual subsites of goose egg white lysozyme to be -0.5, -2.2, $+4.2$, -1.5, -2.6, and -2.8 kcal/mol for subsites -3, -2, -1, $+1$, $+2$, and $+3$, respectively, and the total free energy change of $(GlcNAc)_6$ binding to -3~$+3$ subsites to be 5.4 kcal/mol. The value is very close to that obtained by ITC. Even though multiple modes of binding are possible for $(GlcNAc)_6$, a major fraction of $(GlcNAc)_6$ is likely to bind to subsites -3, -2, -1, $+1$, $+2$ and $+3$.

Comparison with the $(GlcNAc)_n$/g-type lysozyme binding mode determined by X-ray crystallography

As stated in the introductory section, the X-ray crystal structure of g-type lysozymes in a complex with $(GlcNAc)_n$ has been solved by two independent groups (*15*, *16*). The first report was on the goose egg white lysozyme (GEWL) in a complex with $(GlcNAc)_3$, in which the three GlcNAc residues bind to subsites -3, -2 and -1 through hydrogen bonds with Glu73, Asp97, Ser100, His101, Tyr147 and Asn148 (*15*). All of these residues are conserved in OEL, as shown in Fig. 1. The second report was on the g-type lysozyme from Atlantic cod, GLAc (*16*). The crystal structure revealed the binding of $(GlcNAc)_3$ to subsites $+1$, $+2$ and $+3$, in addition to the binding of $(GlcNAc)_2$ to subsites -3 and -2. Asp101(Asp97), His105(His101), Tyr151(Tyr147) and Arg157(Asn153) formed a hydrogen-bond with the -2 sugar and Gly156(Gly152) formed a hydrogen-bond with the -3 sugar (the residues in parentheses are the corresponding residues in OEL; Fig. 1). Arg72(Arg72), Glu73(Glu73), Asp90(Asp86), Gln99(Gln95) and Thr169(Thr165) formed a hydrogen-bond with the $+1$ sugar; Gln23(Pro23) and Arg72(Arg72) with the $+2$ sugar; and Asp24(Glu24), Arg75(His75) and Asn78(Lys78) with the $+3$ sugar. Overall, the binding at subsites -2 and -3 seems quite similar between GEWL and GLAc. The amino acids interacting with the sugar residues determined by X-ray crystallography are summarized in the left column of Table I. On the other hand, NMR titration reveals not only sites of direct interaction, but also sites that are undergoing the conformational change induced by oligosaccharide binding. When $(GlcNAc)_4$ binds to the wild-type OEL, the resonances for Arg99 and Thr165 completely disappeared, and those for Val96, Ser100, Asn148, Ala149 and Gly150 significantly shifted. The NMR result appears to be consistent with the crystal structure. The NMR signals affected by the oligosaccharide

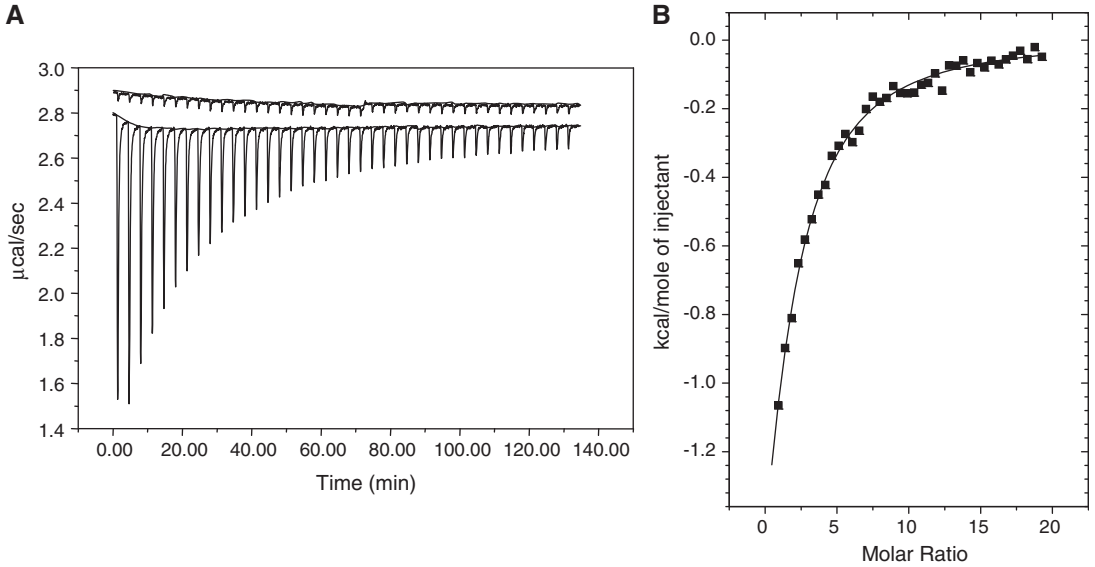

Fig. 6 Isothermal microcalorimetric profile of the titration of the $(GlcNAc)_6$ solution into E73A OEL. Aliquots (7 μl) of 9.65–31.9 mM $(GlcNAc)_n$ in 20 mM sodium acetate buffer, pH 5.0, were added via a 250-μl syringe to a sample cell that contained 1.4482 ml of a stirred (310 rpm) 178–364 μM OEL solution equilibrated at 30°C. (A) The area of each trough corresponds to the heat generated after the addition of 7 μl of $(GlcNAc)_6$ solution to 1.4482 ml of the enzyme solution. (B) Titrating curves obtained by integrating the areas of the troughs in A and normalizing to 1 mol of injected oligosaccharide. The lines are the best fits assuming a single binding site per domain.

binding include the resonances for amino acids directly interacting with the sugar residue, such as Ser100 (subsite −2), Asn148 (subsite −1) and Thr165 (subsite +1), or neighbouring residues probably undergoing conformational change, such as Arg99, Ala149 and Gly150.

NMR titration data of $(GlcNAc)_6$ to E73A OEL provided additional information on the mode of binding to subsites +1, +2 and +3. In addition to the amino acids affected by $(GlcNAc)_4$, the resonances for Ala79 and Asn87 adjacent to the interacting residues, Lys78 (subsite +3) and Asp86 (subsite +1), respectively, were found to be strongly shifted by the binding of $(GlcNAc)_6$. These results suggest that the binding mode obtained by NMR spectroscopy is basically similar to that obtained by X-ray crystallography (*16*). The similarity is clearly seen from Table I, in which the amino acids affected by the $(GlcNAc)_n$ titration are listed together with the X-ray data.

Catalytic residues. It is well known that, in hen egg white lysozyme, the hydrolytic reaction of the β-1-,4-glycosidic linkage takes place through the concerted actions of a proton donor, Glu35, and a catalytic base, Asp52 (*28*). Based on the crystal structure of the GEWL-$(GlcNAc)_3$ complex (*15*), Glu73 has been identified to be a proton donor, because this glutamate is completely superimposed with Glu35 of hen egg white lysozyme. A mutational study by Kawamura *et al*. (*20*) provided direct evidence that Glu73 is a proton donor. However, in GEWL, a second acidic residue (catalytic base) was not found at the position corresponding to that of Asp52 of hen lysozyme. Thus, Weaver *et al*. proposed that the second acidic residue is not essential for the catalytic activity of GEWL. However, this proposal has been controversial for some time. From the crystallographic analysis of GLAc in a complex with $(GlcNAc)_2$+$(GlcNAc)_3$, Helland *et al*. (*16*) found that the two aspartic acids Asp90 and Asp101 (corresponding to Asp86 and Asp97 in OEL and GEWL) are involved in catalysis, and that Asp101 (Asp97 in OEL) is more crucial. In our NMR data, the signal of Asp97 was more responsive to the oligosaccharide binding than that of Asp86. When OEL was saturated with $(GlcNAc)_2$, the $\Delta\delta$ values for the Asp86 and Asp97 signals were 0 and 0.05, respectively; the values were 0.04 and 0.15 upon saturation with $(GlcNAc)_4$, and 0.06 and 0.21 upon saturation with $(GlcNAc)_6$. These data appear to be consistent with the proposal made by Helland *et al*. (*16*); i.e. Asp97 is much more possible to interact with the sugar residue than Asp86. Hirakawa *et al*. (*29*) constructed the modelled structure of GEWL in a complex with $(GlcNAc)_6$, and found a water molecule, which has the potential to enter into the space between the Asp97 carboxyl oxygen and the C1 carbon of the −1 sugar. Thus, they proposed that Asp97 would act as a second carboxylate in the lysozyme catalysis. Our NMR data are also consistent with the findings from the modelling study.

In conclusion, we analysed the mode of binding of $(GlcNAc)_n$ to a g-type lysozyme in solution by NMR spectroscopy. The binding mode of wild-type OEL was basically similar to that determined by X-ray crystallography of GEWL. In E73A OEL, however, we found that the interaction sites for $(GlcNAc)_n$ were more widely spread over the substrate-binding cleft than expected, due to multiple modes of binding. The association constant obtained by NMR spectroscopy was found to be consistent with that obtained by ITC. The site for $(GlcNAc)_4$ binding to E73A OEL appears to be different from that to the wild-type, because of the lack of interaction of Glu73 with the −1 sugar.

Table I. Comparison between amino acid residues forming the substrate-binding cleft (X-ray crystallography) and those affected by $(GlcNAc)_n$ titration (NMR spectroscopy).

	Method	
Subsite	X-ray crystallography	NMR titration with $(GlcNAc)_6$ using OEL
−4		Ala126
−3	His101[a]	–
	Tyr104(Ser100)[b]	Ser100
		Lys102
	Ile119[a]	
		Met123
		Phe131
	Gly156(152)[b]	Gly152
−2		Val96
	Asp97[a], Asp101(97)[b]	Asp97
		Arg98
		Arg99
	Ser100[a], Tyr104(Ser100)[b]	Ser100
	His101[a], His105(101)[b]	
	Phe127[a]	Phe127
	Tyr147[a], Tyr151(147)[b]	
		Ala149
	Gly154(150)[b]	Gly150
	Arg157(153)[b]	
−1	Glu73[a]	Glu73
		Arg98
	Asn148[a]	Asn148
+1	Arg72[b]	Arg72
	Glu73[b]	
	Val79[b]	Ala79
	Ile80[b]	
		Trp84
	Gly89(85)[b]	Gly85
	Asp90(86)[b]	Asp86
		Asn87
		Gly88
		Asn89
		Gly90
	Gln99(95)[b]	Gln95
	–	Ile162
	Thr169(165)[b]	Thr165
		Asp172
+2	Glu23(Pro23)[b]	Ser17
+3		Ser17
	Asp24[b]	
		Arg72
	Arg75[b]	His75
	Asn78[b]	Lys78
		Ala79

[a]GEWL [Weaver *et al.* (*15*)], molecular model GEWL-$(GlcNAc)_6$ (*29*). [b]Atlantic cod lysozyme [Helland *et al.* (*16*)].

Supplementary Data

Supplementary Data are available at *JB* online.

Conflict of interest
None declared.

References

1. Jollès, P. and Jollès, J. (1984) What's new in lysozyme research? Always a model system, today as yesterday. *Mol. Cell Biochem.* **63**, 165–189
2. Chipman, D.M., Pollock, J.J., and Sharon, N. (1968) Lysozyme-catalyzed hydrolysis and transglycosylation reactions of bacterial cell wall oligosaccharides. *J. Biol. Chem.* **243**, 487–496
3. Banerjee, S.K., Holler, E., Hess, G.P., and Rupley, J.A. (1975) Reaction of *N*-acetylglucosamine oligosaccharides with lysozyme. Temperature, pH, and solvent deuterium isotope effects; equilbrium, steady state, and pre-steady state measurements. *J. Biol. Chem.* **250**, 4355–4367
4. Masaki, A., Fukamizo, T., Otakara, A., Torikata, T., Hayashi, K., and Imoto, T. (1981) Lysozyme-catalyzed reaction of chitooligosaccharides. *J. Biochem.* **90**, 527–533
5. Fukamizo, T., Torikata, T., Kuhara, S., and Hayashi, K. (1982) Human lysozyme-catalyzed reaction of chitooligosaccharides. *J. Biochem.* **92**, 709–716
6. Fukamizo, T., Torikata, T., Nagayama, T., Minematsu, T., and Hayashi, K. (1983) Enzymatic activity of avian egg-white lysozymes. *J. Biochem.* **94**, 115–122
7. Mirelman, D., Kleppe, G., and Jensen, H.B. (1975) Studies on the specificity of action of bacteriophage T4 lysozyme. *Eur. J. Biochem.* **55**, 369–373
8. Jensen, H.B., Kleppe, G., Schindler, M., and Mirelman, D. (1976) The specificity requirements of bacteriophage T4 lysozyme. *Eur. J. Biochem.* **66**, 319–325
9. Arnheim, N., Inouye, M., Law, L., and Laudin, A. (1973) Chemical studies on the enzymatic specificity of goose egg white lysozyme. *J. Biol. Chem.* **248**, 233–236
10. Kuroki, R., Morimoto, K., and Matthews, B.W. (1998) Converting T4 phage lysozyme into a transglycosidase. *Ann. NY Acad. Sci.* **864**, 362–365
11. Fukamizo, T., Minematsu, T., Yanase, Y., Hayashi, K., and Goto, S. (1986) Substrate size dependence of lysozyme-catalyzed reaction. *Arch. Biochem. Biophys.* **250**, 312–321
12. Henrissat, B. and Bairoch, A. (1993) New families in the classification of glycosyl hydrolases based on amino acid sequence similarities. *Biochem. J.* **293**, 781–788
13. Monzingo, A.F., Marcotte, E.M., Hart, P.J., and Robertus, J.D. (1996) Chitinases, chitosanases, and lysozymes can be divided into procaryotic and eucaryotic families sharing a conserved core. *Nat. Struct. Biol.* **3**, 133–140
14. Weaver, L.H., Grütter, M.G., Remington, S.J., Gray, T.M., Isaacs, N.W., and Matthews, B.W. (1984–1985) Comparison of goose-type, chicken-type, and phage-type lysozymes illustrates the changes that occur in both amino acid sequence and three-dimensional structure during evolution. *J. Mol. Evol.* **21**, 97–111
15. Weaver, L.H., Grütter, M.G., and Matthews, B.W. (1995) The refined structures of goose lysozyme and its complex with a bound trisaccharide show that the "goose-type" lysozymes lack a catalytic aspartate residue. *J. Mol. Biol.* **245**, 54–68
16. Helland, R., Larsen, R.L., Finstad, S., Kyomuhendo, P., and Larsen, A.N. (2009) Crystal structures of g-type lysozyme from Atlantic cod shed new light on substrate binding and the catalytic mechanism. *Cell Mol. Life Sci.* **66**, 2585–2598
17. Honda, Y. and Fukamizo, T. (1998) Substrate binding subsites of chitinase from barley seeds and lysozyme from goose egg white. *Biochim. Biophys. Acta.* **1388**, 53–65
18. Kawamura, S., Fukamizo, T., Araki, T., and Torikata, T. (2003) Expression of a synthetic gene coding for ostrich egg-white lysozyme in *Pichia pastoris* and its enzymatic activity. *J. Biochem.* **133**, 123–131
19. Schoentgen, F., Jolle's, J., and Jolle's, P. (1982) Complete amino acid sequence of ostrich (*Struthio camelus*) egg-white

lysozyme, a goose type lysozyme. *Eur. J. Biochem.* **123**, 489–497

20. Kawamura, S., Ohno, K., Ohkuma, M., Chijiiwa, Y., and Torikata, T. (2006) Experimental verification of the crucial roles of Glu73 in the catalytic activity and structural stability of goose-type lysozyme. *J. Biochem.* **140**, 75–85
21. Kawamura, S., Ohkuma, M., Chijiiwa, Y., Kohno, D., Nakagawa, H., Hirakawa, H., Kuhara, S., and Torikata, T. (2008) Role of disulfide bonds in goose-type lysozyme. *FEBS J.* **275**, 2818–2830
22. Wishart, D.S., Bigam, C.G., Holm, A., Hodges, R.S., and Sykes, B.D. (1995) ^{1}H, ^{13}C and ^{15}N random coil NMR chemical shifts of the common amino acids. I. Investigations of nearest-neighbor effects. *J. Biomol. NMR* **5**, 67–81
23. Delaglio, F., Grzesiek, S., Vuister, G. W., Zhu, G., Pfeifer, J., and Bax, A. (1995) NMRPipe: a multidimensional spectral processing system based on UNIX pipes. *J. Biol. NMR.* **6**, 277–293
24. Goddard, T.D. and Kneller D.G. SPARKY 3, University of California, San Francisco
25. Wiseman, T., Williston, S., Brandts, J.F., and Lin, L.-N. (1989) Rapid measurement of binding constants and heats of binding using a new titration calorimeter. *Anal. Biochem.* **179**, 131–137
26. Jelesarov, I. and Bosshard, H.R. (1999) Isothermal titration calorimetry and differential scanning calorimetry as complementary tools to investigate the energetics of biomolecular recognition. *J. Mol. Recognit.* **12**, 3–18
27. Pierce, M.M., Raman, C.S., and Nall, B.T. (1999) Isothermal titration calorimetry of protein-protein interactions. *Methods.* **19**, 213–221
28. Imoto, T., Johnson, L.N., North, A.C.T., Phillips, D.C., and Rupley, J.A. (1972) Vertebrate lysozyme, in *The Enzymes* Vol. 7, 3rd edn (Boyer, P.D., ed.), pp. 665–868, Academic Press, New York
29. Hirakawa, H., Ochi, A., Kawahara, Y., Kawamura, S., Torikata, T., and Kuhara, S. (2008) Catalytic reaction mechanism of goose egg-white lysozyme by molecular modeling of enzyme-substrate complex. *J. Biochem.* **144**, 753–761